

# Kinetics in one-dimensional lattice gas and Ising models from time-dependent density functional theory

M. Kessler, W. Dieterich, and P. Maass  
*Fachbereich Physik Universität Konstanz, D-78457 Konstanz, Germany*

H.L. Frisch,  
*Dept. of Chemistry, SUNY at Albany, Albany NY 12222, USA*

J.F. Gouyet  
*Laboratoire de Physique de la Matière Condensée Ecole Polytechnique, 91128 Palaiseau Cedex, France*  
(Dated: January 23, 2002)

Time-dependent density functional theory, proposed recently in the context of atomic diffusion and non-equilibrium processes in solids, is tested against Monte Carlo simulation. In order to assess the basic approximation of that theory, the representation of non-equilibrium states by a local equilibrium distribution function, we focus on one-dimensional lattice models, where all equilibrium properties can be worked exactly from the known free energy as a functional of the density. This functional determines the thermodynamic driving forces away from equilibrium. In our studies of the interfacial kinetics of atomic hopping and spin relaxation, we find excellent agreement with simulations, suggesting that the method is useful also for treating more complex problems.

PACS numbers: 05.10.Gg,31.15.Ew,05.60.Cd,66.30.Dn

## I. INTRODUCTION

Establishing a link between macroscopic laws of diffusion and relaxation with a microscopic master equation for atomic degrees of freedom has remained a fundamental problem in non-equilibrium statistical mechanics. Moreover, numerous examples exist in metallurgy, semiconductor device technology, glass science and polymer science, where control over the time-development of microstructures is crucial in the design of materials with special mechanical, electrical and magnetic properties. Hence there is a need also from a practical viewpoint to derive tractable kinetic equations incorporating specific materials properties, so that processes like nucleation, spinodal decomposition and magnetic relaxation can be treated in a realistic manner.

The simplest approach is to study mean-field kinetic equations, derived from the master equation by neglecting any atomic correlation effects [1, 2, 3]. Such equations suffer from the obvious drawback that their stationary solutions yield the mean-field phase diagram, which may differ even qualitatively from the correct phase diagram. Several routes for improvement have been proposed in the literature, including the path probability method [4, 5], effective Hamiltonian methods [6] or time-dependent density functional theory (TDFT) [7, 8, 9]. The latter approach implements the idea of local equilibrium and leads to thermodynamic driving forces which in principle are derived from an exact free energy functional. Density functional theories are normally formulated for continuous fluid systems [10], but adaptation to discrete lattice systems is straightforward [11, 12]. In this way one can obtain generalized mean-field kinetic equations for single-particle or single-spin densities which in principle are consistent with the exact equilibrium properties.

If necessary, additional approximations with respect to equilibrium quantities can be carried out in a separate step.

The above-mentioned kinetic theories mostly focus on purely dissipative processes in discrete lattice systems. For fluid systems, the derivation of nonlinear transport equations for hydrodynamic variables is a more complicated subject. Some generalizations of Moris' well-known projection operator technique and mode coupling approximations to situations far away from equilibrium [13, 14] have been applied, for example, to problems of nonlinear hydrodynamics, the glass transition [15] and to granular flows [16].

Our aim in this paper is to apply the TDFT scheme to purely dissipative "conserved" atomic migration and "non-conserved" spin dynamics processes in one-dimensional lattice models for which the exact free energy functional is known. This enables us to separate out and to test the local equilibrium assumption against Monte Carlo simulation. Specifically, we study the temporal evolution of domains with different ordering, and of the associated interface. It is demonstrated that in these problems the TDFT shows remarkable quantitative accuracy, suggesting that this method may be useful also under more general conditions.

In section 2 we briefly recall our basic approach. Section 3 starts out with an exact free energy functional for a one-dimensional lattice and provides expressions for local correlators in terms of particle densities. With these results we arrive at a closed system of kinetic equations on the single-particle level. Following the classification by Hohenberg and Halperin [17] these equations take the form of generalized "model B" or "model A" equations in cases of a conserved or a non-conserved order parameter, respectively. Solving these equations, we subsequently

discuss the time–evolution of an initially sharp interface between two differently ordered domains in both of these cases (section 4). Excellent agreement with Monte Carlo simulations is found, in contrast to ordinary mean–field (MF) theory which produces substantial deviations.

## II. OVERVIEW OF TIME–DEPENDENT DENSITY FUNCTIONAL THEORY (TDFT) FOR STOCHASTIC LATTICE SYSTEMS

### A. Atomic hopping

Let us begin with hopping of particles on a lattice of equivalent sites  $i$ , which are either simply occupied ( $n_i = 1$ ) or vacant ( $n_i = 0$ ), so that occupation numbers satisfy  $n_i^2 = n_i$ . The hopping process is described by a master equation for probabilities  $P(\mathbf{n}, t)$  of finding an occupational configuration  $\mathbf{n} \equiv \{n_i\}$  at time  $t$ . As elementary steps we assume moves of a single particle from an occupied site to a vacant nearest neighbor site. The associated rates  $w_{i,k}(\mathbf{n})$  for adjacent sites  $i$  and  $k$  to exchange their occupation satisfy the detailed balance condition with respect to a given lattice gas Hamiltonian  $H(\mathbf{n})$ .

A detailed description of TDFT is found in Ref. [8]. Hence we need to recall only the main steps, and add some remarks as to their physical content. The basic approximation is to replace the distribution  $P(\mathbf{n}, t)$  by the local equilibrium distribution

$$P^{loc}(\mathbf{n}, t) = \frac{1}{Z(t)} \exp \left\{ -\beta \left[ H(\mathbf{n}) + \sum_i h_i(t) n_i \right] \right\}, \quad (1)$$

where deviations from equilibrium are represented in terms of time–dependent single–particle fields  $\mathbf{h}(t) = \{h_i(t)\}$ .  $Z(t)$  is a normalization factor, which at equilibrium ( $\mathbf{h}(t) = 0$ ) reduces to the canonical partition function. Requiring self–consistency on the single–particle level allows us to eliminate  $\mathbf{h}(t)$  in favor of mean occupation numbers  $\mathbf{p}(t) = \{p_i(t)\}$  with  $p_i(t) = \langle n_i \rangle_t$ , where  $\langle \dots \rangle_t$  denotes an average with respect to the distribution (1). In this way a closed system of equations for  $\mathbf{p}(t)$  can be derived.

To carry through this program we start from the equation of continuity which follows directly from the original master equation. Replacement of exact averages by local equilibrium averages gives

$$\frac{dp_i(t)}{dt} + \sum_k \langle j_{i,k} \rangle_t = 0, \quad (2)$$

with known expressions [8] for the current  $j_{i,k}(\mathbf{n})$  from site  $i$  to site  $k$  in terms of  $w_{i,k}(\mathbf{n})$ . Notice that at any instant of time the exponent in (1) describes an inhomogeneous lattice gas which involves a spatially varying single–particle potential  $\mathbf{h}(t)$ . Hence, calculation of averages from (1) is precisely the kind of problem treated

by density functional theory (DFT) in classical statistical mechanics. There, one considers a class of systems with fixed interactions and arbitrary single–particle potentials, specified here by  $H(\mathbf{n})$  and  $\mathbf{h}$ , respectively. Averaged occupation numbers and correlation functions are determined from derivatives of a free energy functional  $F(\mathbf{p})$  associated with the Hamiltonian  $H(\mathbf{n})$ . Specifically,  $\mathbf{p}(t)$  is determined by the set of equations

$$h_i(t) + \mu_i(\mathbf{p}(t)) = \mu_{tot}, \quad (3)$$

with  $\mu_{tot}$  the overall chemical potential, and

$$\mu_i(\mathbf{p}) = \partial F(\mathbf{p}) / \partial p_i, \quad (4)$$

the local chemical potential as functional of  $\mathbf{p}$ . Much experience has been gained during the last two decades how to construct  $F(\mathbf{p})$  from a given Hamiltonian  $H(\mathbf{n})$ . In the subsequent considerations we therefore assume  $F(\mathbf{p})$  to be known. Since in the framework of DFT occupational correlation functions are functionals of  $\mathbf{p}$ , we can formally regard (2) as the desired closed set of equations for  $\mathbf{p}(t)$ .

In order to make this procedure explicit and to establish a connection with thermodynamic driving forces, we again recall Ref. [8] where it is shown that the average current can be written as

$$\langle j_{i,k} \rangle_t = M_{i,k}(t) [A_i(t) - A_k(t)]. \quad (5)$$

The quantities

$$A_i(t) = \exp[\beta \mu_i(\mathbf{p}(t))] \quad (6)$$

are local activities, whose discrete gradient (along the bond connecting  $i$  and  $k$ ) plays the role of a thermodynamic force that drives the current. The quantity

$$M_{i,k}(t) = \frac{1}{2} \langle w_{i,k}(\mathbf{n}) \exp[\beta(h_i(t)n_i + h_k(t)n_k)] \rangle_t, \quad (7)$$

where  $M_{i,k}(t) = M_{k,i}(t)$ , is a mobility coefficient that depends on the actual nonequilibrium state. Further discussion of (7) simplifies when we choose the hopping rates  $w_{i,k}(\mathbf{n})$  such that they depend only on the energy in the initial state, i. e.

$$w_{i,k}(\mathbf{n}) = \alpha [n_i(1 - n_k)e^{\beta H_i} + n_k(1 - n_i)e^{\beta H_k}]. \quad (8)$$

The first term describes hopping from  $i$  to  $k$ , with a thermally activated rate determined by the interaction energy  $H_i$  of a particle at site  $i$  with its environment.  $\alpha$  is some bare rate constant. The reverse hopping process is described by the second term in (8). With this expression for  $w_{i,k}(\mathbf{n})$ , one can show [8] that Eq. (7) transforms into

$$M_{i,k}(t) = \alpha \langle (1 - n_i)(1 - n_k) \rangle_t. \quad (9)$$

At this stage,  $M_{i,k}(t)$  does no longer explicitly depend on  $\mathbf{h}$ . Physically, equation (9) tells us that the mobility coefficient based on (8) is given by the nearest–neighbor vacancy correlator.

It should be kept in mind that in this TDFT–scheme all deviations from equilibrium are described in a mean–field manner in the sense that the underlying distribution function (1) deviates from the canonical distribution merely by single–particle terms. Relationships between occupational correlators and densities  $\mathbf{p}(t)$ , which enter this theory, are local in time and are given by the equilibrium theory. This implies the assumption that correlators relax fast to their local equilibrium values, compared with time scales characterizing the evolution of  $\mathbf{p}(t)$ . Ordinary kinetic mean–field theory is recovered when we use mean–field expressions for  $\mu_i(\mathbf{p})$  and replace (9) by  $M_{i,k}^{MF}(t) = \alpha(1-p_i(t))(1-p_k(t))$ . By contrast, in TDFT the local chemical potential appearing in (6) is defined by the exact chemical potential functional so that (2) together with (5) describes relaxation towards the exact equilibrium state. Moreover, the expression (9) for the mobility preserves local correlation effects in the jump dynamics.

## B. Spin relaxation

To exemplify the dynamics of a non–conserved order parameter, we study spin–relaxation in a kinetic Ising model. Elementary transitions in the underlying master equation are supposed to be individual spin flips  $\sigma_i \rightarrow -\sigma_i$ , where  $\sigma_i = \pm 1$ . By  $w_i(\boldsymbol{\sigma})$  we denote the associated rate in an initial spin configuration  $\boldsymbol{\sigma}$ . The local equilibrium distribution  $P^{(loc)}(\boldsymbol{\sigma}, t)$  is analogous to (1). It involves the Ising Hamiltonian  $H(\boldsymbol{\sigma})$  supplemented by time–dependent magnetic fields  $\mathbf{h}(t)$ , which couple to the spins in the form  $-\sum_i h_i(t)\sigma_i$ . As shown in the Appendix, the equations of motion read

$$\frac{d\langle\sigma_i\rangle_t}{dt} = -\Gamma_i(t) \sinh \beta \left( \frac{\partial F(\langle\boldsymbol{\sigma}\rangle_t)}{\partial\langle\sigma_i\rangle_t} - h \right), \quad (10)$$

with kinetic coefficients

$$\Gamma_i(t) = 2\langle w_i(\boldsymbol{\sigma})e^{-\beta h_i(t)\sigma_i} \rangle_t, \quad (11)$$

$F$  is the intrinsic free energy functional associated with the exchange interaction, and  $h$  an overall constant magnetic field. Equation (10) again displays the exact thermodynamic driving force in the spirit of TDFT. It can be regarded as a generalized “model A” equation in the classification by Hohenberg and Halperin [17], whereas Eqs. (2), (5) and (6) constitute generalized “model B” equations. Note that sufficiently close to equilibrium one can ignore  $\mathbf{h}(t)$  in (11) and linearize the sinh–term in (10) to obtain  $d\langle\sigma_i\rangle_t/dt \simeq -2\beta\langle w_i(\boldsymbol{\sigma}) \rangle_{eq}(\partial F/\partial\langle\sigma_i\rangle_t - h)$ . The kinetic coefficient is then simply given by the equilibrium spin flip rate  $\langle w_i(\boldsymbol{\sigma}) \rangle_{eq}$ .

## C. Consistency with thermodynamics

Finally it is easy to show that our evolution equations are consistent with the second law of thermodynamics:

The total free energy decreases monotonously with time until the equilibrium condition is satisfied. For hopping, the rate of change of the free energy is given by

$$\begin{aligned} \frac{dF}{dt} &= \sum_i \frac{\partial F}{\partial p_i} \frac{dp_i}{dt} \\ &= -k_B T \sum_{i,k} M_{i,k} x_i (e^{x_i} - e^{x_k}) \\ &= -\frac{k_B T}{2} \sum_{i,k} M_{i,k} (x_i - x_k) (e^{x_i} - e^{x_k}) \leq 0, \quad (12) \end{aligned}$$

where we have used (2), (5) and (6) together with the abbreviation  $\partial(\beta F/\partial p_i) = x_i$ , and  $M_{i,k} = M_{k,i}$ . Currents through the boundaries of the system are supposed to be zero. The inequality in (12) arises from  $M_{i,k} > 0$ , see (7), and from  $(x-y)(e^x - e^y) > 0$  for  $x \neq y$ . The equality sign in (12) holds if and only if  $x_i = x_k$  for all  $i$  and  $k$ , which means that  $\mu_i = \text{const}$ .

Similarly, for the kinetic Ising spin model, the total free energy including the coupling to the external field  $h$  satisfies

$$\frac{d}{dt} \left( F - h \sum_i \sigma_i \right) = -k_B T \sum_k \Gamma_k x_k \sinh x_k \leq 0, \quad (13)$$

where  $x_k = \beta(\partial F/\partial\langle\sigma_k\rangle_t - h)$ . The inequality follows because  $\Gamma_k > 0$  (see (11)) and  $x \sinh x > 0$  for  $x \neq 0$ . Equation (13) becomes an equality if  $\partial F/\partial\langle\sigma_k\rangle_t = h$  for all  $k$ .

## III. ONE DIMENSION: EXACT FUNCTIONALS

To test the local equilibrium distribution (1) it is desirable to avoid any approximation with respect to static properties. This can be achieved by using exact free energy functionals, which are available for certain one–dimensional systems [18, 19, 20].

### A. Atomic hopping

For a lattice gas with nearest neighbor interactions on a linear chain of sites  $i$ ;  $1 \leq i \leq M$ ; with occupied boundary sites at  $i = 0$  and  $i = M+1$ , the free energy functional reads [19]

$$\begin{aligned} F\{\mathbf{p}\} = V \sum_{i=0}^M p_{i+1,i}^{(1)} + k_B T \sum_{i=0}^{M-1} \left[ \sum_{n=1}^4 p_{i+1,i}^{(n)} \ln p_{i+1,i}^{(n)} - p_i \ln p_i \right. \\ \left. - (1-p_i) \ln(1-p_i) \right], \quad (14) \end{aligned}$$

where  $V$  denotes the interaction constant, and  $p_{i+1,i}^{(n)}$  with  $n = 1, \dots, 4$  are the two–point correlators for the four

possibilities of particles and holes on site  $i$  and site  $i + 1$ ,

$$\begin{aligned}
p_{i+1,i}^{(1)} &= \langle n_{i+1}n_i \rangle, \\
p_{i+1,i}^{(2)} &= \langle (1 - n_{i+1})n_i \rangle = p_i - p_{i+1,i}^{(1)}, \\
p_{i+1,i}^{(3)} &= \langle n_{i+1}(1 - n_i) \rangle = p_{i+1} - p_{i+1,i}^{(1)}, \\
p_{i+1,i}^{(4)} &= \langle (1 - n_{i+1})(1 - n_i) \rangle = 1 - p_i - p_{i+1} + p_{i+1,i}^{(1)}.
\end{aligned} \tag{15}$$

From the techniques of Ref. [19] it follows that

$$p_{i+1,i}^{(1)} p_{i+1,i}^{(4)} = p_{i+1,i}^{(2)} p_{i+1,i}^{(3)} e^{-\beta V}, \tag{16}$$

a relation, which is equivalent to the quasi-chemical approach. Given these relations, it turns out that  $\partial F / \partial p_{i+1,i}^{(1)} = 0$ . This suggests that  $F$  may be minimized also with respect to correlators in cases where these cannot be calculated explicitly.

The boundary conditions for the correlators are  $p_{1,0}^{(1)} = p_1$  and  $p_{M+1,M}^{(1)} = p_M$ . For  $1 \leq i \leq M - 1$ , combination of (15) with (16) yields a quadratic equation for  $p_{i+1,i}^{(1)}$ . In this way the representation of  $p_{i+1,i}^{(n)}$  as functionals of  $\mathbf{p}$  is completed. The fact that  $p_{i+1,i}^{(n)}$  only depends on  $p_{i+1}$  and  $p_i$  clearly is a special feature in one dimension.

The kinetic equations derived in section 2 are now combined with (14). Evidently, from (9),

$$M_{i,i+1}(t) = \alpha p_{i+1,i}^{(4)}, \tag{17}$$

while the local chemical potential is found to satisfy

$$\beta \mu_i = \ln \frac{p_{i+1,i}^{(2)} p_{i,i-1}^{(3)}}{p_{i+1,i}^{(4)} p_{i,i-1}^{(4)}} - \ln \frac{p_i}{1 - p_i}. \tag{18}$$

From (5), (17) and (18) we obtain for the current

$$\begin{aligned}
\langle j_{i,i+1} \rangle_t &= \alpha \left[ \frac{p_{i,i-1}^{(3)} (1 - p_i)}{p_i} \frac{p_{i+1,i}^{(2)}}{p_{i,i-1}^{(4)}} \right. \\
&\quad \left. - \frac{p_{i+2,i+1}^{(2)} (1 - p_{i+1})}{p_{i+1}} \frac{p_{i+1,i}^{(3)}}{p_{i+2,i+1}^{(4)}} \right].
\end{aligned} \tag{19}$$

In these last equations (17)–(19), densities and correlators are local equilibrium quantities. The final form of our kinetic equations as a nonlinear set of differential equations for  $p_i(t)$  emerges when we reexpress  $p_{i+1,i}^{(n)}$  in terms of  $p_{i+1}$  and  $p_i$  in the way described above.

For comparison we also consider the ordinary mean-field equations. These are obtained by factorizing all correlators in (18) and (19), for example  $p_{i+1,i}^{(1)} \simeq p_{i+1} p_i$ . The mean-field current is then found as

$$\begin{aligned}
\langle j_{i,i+1}^{MF} \rangle_t &= \alpha \{ p_i - p_{i+1} + K [ p_{i-1} p_i (1 - p_{i+1}) \\
&\quad - (1 - p_i) p_{i+1} p_{i+2} ] \}
\end{aligned} \tag{20}$$

with  $K = \exp(\beta V) - 1$ .

## B. Spin relaxation

Next we turn to spin relaxation in the linear Ising model. Rather than using (10) we immediately choose transition rates

$$w_i(\boldsymbol{\sigma}) = \frac{\alpha}{2} \left( 1 - \frac{\gamma}{2} \sigma_i (\sigma_{i+1} + \sigma_{i-1}) \right) (1 - \delta \sigma_i) \tag{21}$$

and start from the evolution equations for single spins as given in the original work by Glauber [21],

$$\begin{aligned}
\frac{d\langle \sigma_i \rangle_t}{dt} &= \alpha \left[ \langle \sigma_i \rangle_t - \frac{\gamma}{2} (\langle \sigma_{i+1} \rangle_t + \langle \sigma_{i-1} \rangle_t) - \delta \right. \\
&\quad \left. + \frac{\delta \gamma}{2} (\langle \sigma_{i+1} \sigma_i \rangle_t + \langle \sigma_i \sigma_{i-1} \rangle_t) \right].
\end{aligned} \tag{22}$$

Here,  $\gamma = \tanh 2\beta J$  and  $\delta = \tanh \beta h$ , where  $J > 0$  denotes the (ferromagnetic) nearest-neighbor exchange coupling and  $h$  a constant external magnetic field. It is well known that for  $h = 0$  these equations become linear and easily soluble. By contrast, for  $h \neq 0$ , the appearance of correlators  $\langle \sigma_{i+1} \sigma_i \rangle_t$  in (22) prevents us from obtaining an exact solution. Using the well-known representation of Ising spin variables by occupation numbers,  $\sigma_i = 2n_i - 1$ , and vice versa, we can treat the correlators  $\langle \sigma_{i+1} \sigma_i \rangle$  in perfect analogy to  $\langle n_{i+1} n_i \rangle$ . In particular, Eq. (16) with  $J = 4V$  transforms into a quadratic equation for  $\langle \sigma_{i+1} \sigma_i \rangle$ , whose solution, expressed in terms of  $\langle \sigma_{i+1} \rangle$  and  $\langle \sigma_i \rangle$ , is substituted into (22). This yields our TDFT-equation of motion for spins. Likewise, we obtain from (16) the free energy as functional of the spin density, which could be used in (10).

## IV. APPLICATION TO INTERFACIAL KINETICS

We now apply the TDFT to problems of the time-evolution of an initially sharp interface between differently ordered domains on a linear chain. Our purpose is to present a quantitative comparison with both Monte Carlo simulation and simple MF-theory with respect to density profiles, spin-density profiles and the respective correlators.

### A. Atomic hopping

The length of the chain is taken as  $M = 10^3$ . As mentioned before, boundary sites have fixed occupation  $p_0 = p_{M+1} = 1$ . Symmetrical initial conditions at  $t = 0$  are chosen such that we have a vacant region centered around the midpoint of the system,  $p_i(0) = 0$  for  $250 < i < 750$ , and complete occupation in the complementary space. For  $t > 0$ , the initially sharp density profile will progressively broaden due to diffusion. This is shown in Fig. 1 for  $0 \leq i \leq 500$  in the case of a repulsive interaction with  $\beta V = 3$ . Generally, the shape

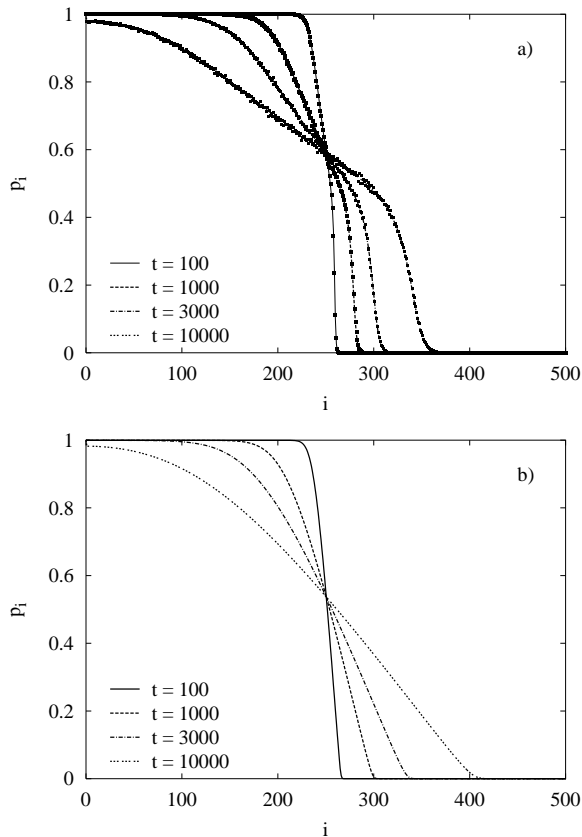


FIG. 1: Comparison of time-dependent density profiles  $p_i$  in the case of hopping dynamics with repulsive interaction  $\beta V = 3$ , obtained from different methods. a) TDFT (lines) and MC simulation (data points) b) Kinetic MF-theory.

of profiles depends on how the interaction enters the elementary hopping rates. Our choice (8) implies that in regions with densities  $p \gtrsim 0.5$  a particle next to a vacant target site has a large chance to be repelled by another particle and hence will assume a large jump rate. By contrast, the repulsion will be less active in dilute regions. This explains the asymmetry of the profiles in Fig. 1a, with a steep drop towards the empty region. The main conclusion from Fig. 1a is the perfect agreement between profiles from TDFT, shown by the full lines, and from Monte Carlo (MC) simulation (data points) [22]. To get smooth profiles from simulation, we took averages over  $10^4$  Monte Carlo runs. By contrast, the MF-profiles in Fig. 1b are more symmetric and deviate significantly from those in Fig. 1a.

For diffusion processes on (continuous) length scales  $x$  and time scales  $t$  much larger than the elementary hopping distance and residence time, we expect the density to depend only on the scaling variable  $\eta = x/(2\sqrt{t})$ , provided the initial conditions can be expressed in terms of  $\eta$ . This is verified in Fig. 2a which shows master-curves  $p(\eta)$  obtained from the profiles in Fig. 1 for different times. In this analysis the origin of the  $x$ -axis is chosen to coin-

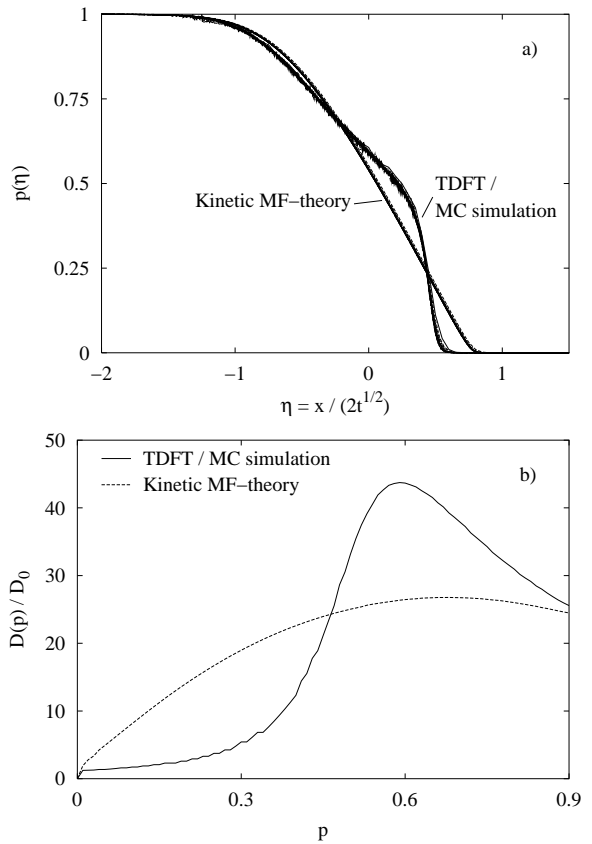


FIG. 2: a) Density profiles shown in Fig. 1 for different times against the scaling variable  $\eta = x/(2\sqrt{t})$ . The length  $x$  in units of the lattice constant and  $t$  in units of  $\Delta t$ , see footnote [22]. b) Concentration-dependent diffusion coefficients  $D(p)$  extracted from the master-curves of Fig. 2a by the Boltzmann-Matano method. (The normalization factor  $D_0$  is the single-particle diffusion constant for infinite dilution.)

cide with the initial density drop at  $i = 250$ . As expected from Fig. 1, the TDFT master-curve, in contrast to MF-theory, practically coincides with the Monte Carlo master-curve.

These results can be analyzed further by the Boltzmann-Matano method [25], which assumes a diffusion equation of the form  $\partial p/\partial x = \partial/\partial x(D(p(x))\partial p/\partial x)$  to hold. From the master-curve  $p(\eta)$  the concentration-dependent diffusion coefficient  $D(p)$  can be deduced according to

$$D(p) = -\frac{2}{(dp/d\eta)} \int_0^p \eta(p') dp', \quad (23)$$

where  $\eta(p)$  is the inverse function of  $p(\eta)$ . The integral can be calculated accurately from the profile of Fig. 2a up to  $p \simeq 0.9$ , and the results for  $D(p)$  are shown in Fig. 2b. Using the MF profile, we recover the  $p$ -dependence of the mean-field diffusion constant. This quantity is calculated easily by separating from the current (20) a factor  $p_{i+1} - p_i$ , i. e. a discrete gradient of the density, and identifying

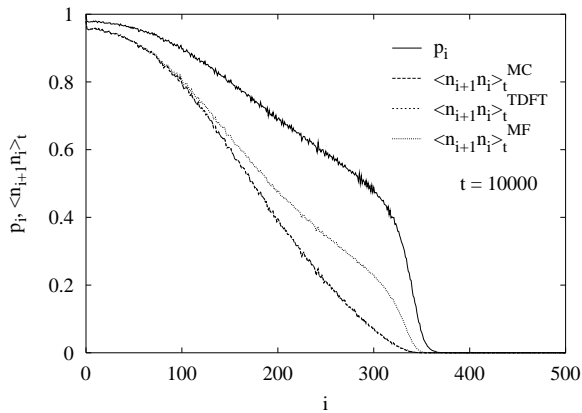


FIG. 3: Correlators  $\langle n_{i+1}n_i \rangle_t$  at  $t = 10^4$  from MC-simulation compared to correlators computed from TDFT and MF-theory, using the same Monte Carlo density profile  $p_i$  (upper curve) as input. The TDFT-correlators are indistinguishable from MC-correlators in this plot.

the result with Ficks' law. One obtains

$$D^{MF}(p) = D_0(1 + K[p^2 + 4p(1 - p)]), \quad (24)$$

with  $D_0 = \alpha a^2$ ,  $a$  being the lattice spacing. The expression (24) shows a broad maximum around  $p = 2/3$ , which reflects the average effect of the repulsion of particles. The TDFT-diffusion constant, however, shows a much sharper maximum. Moreover, when  $p$  becomes small, it approaches the value  $D_0$  more rapidly, and thus gives rise to the steepening of the density profile in the regime  $p \lesssim 0.4$ , as observed in Fig. 2a. This is a correlation effect: In a dilute system, a fast hop of a particle due to the repulsion by a neighboring particle is a rare event because nearest neighbor pairs get suppressed,  $\langle n_{i+1}n_i \rangle < p_{i+1}p_i$ , and hence diffusion is slowed down relative to the MF-prediction. This argument is supplementary to our previous discussion of Fig. 1a.

At this point we remark that such correlations induced by the repulsion of particles are taken into account to a certain extent even by MF-theory when applied to a two-sublattice structure. Density profiles and effective diffusion coefficients calculated in this way in a previous study [23] indeed are similar to those of the present TDFT calculation shown in Fig. 2a and 2b, respectively.

Because of the important role played by the correlators in TDFT it is of interest to make a direct comparison with correlators obtained from Monte Carlo simulation. Fig. 3 exemplifies perfect agreement between those of TDFT and simulation, whereas MF-correlators, calculated here as product  $p_{i+1}p_i$  of the simulated densities, are significantly larger when the densities are small.

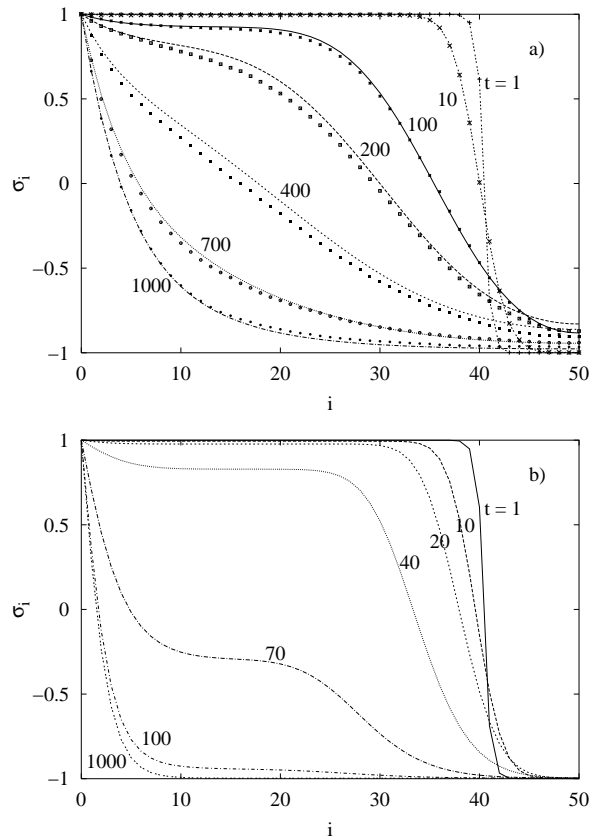


FIG. 4: Comparison of time-dependent spin density profiles in the Glauber model with  $\beta J = 2$  and  $\beta h = -0.1$ , obtained from different methods. a) TDFT (lines) and MC-simulation (data points) b) Kinetic MF-theory

## B. Spin relaxation

In our study of “non-conserved” dynamics in the one-dimensional Glauber model [21] we choose a chain of length  $M = 10^2$  and fixed upward spins at the boundaries,  $\sigma_0 = \sigma_{M+1} = 1$ . Our initial condition at  $t = 0$  now is  $\sigma_i = -1$  for  $40 \leq i \leq 60$  and  $\sigma_i = +1$  for the remaining spins. Notice that in the case  $h = 0$  simple MF-theory in the spirit of this work becomes exact because the correlators in (22) drop out. To depart from this trivial situation we introduce a small field with  $\beta h = -0.1$  which favors downward spin orientation. Spin density profiles in the region  $0 \leq i \leq 50$  for  $\beta J = 2$  at different times  $t > 0$  are presented in Fig. 4a, where the full lines correspond to TDFT, and data points to simulation. The agreement is very good, although not perfect. Generally, the spins in the interior of the system relax towards the equilibrium in the external field. Spins near the boundary are expected to relax towards an equilibrium profile which decays from the boundary ( $\sigma_0 = 1$ ) towards the interior ( $\sigma_i \approx -1$ ) on a length given by the correlation length  $\xi$ . For the temperature considered,  $\xi \simeq 5a$ . During the course of this relaxation, simple MF-theory, based on a

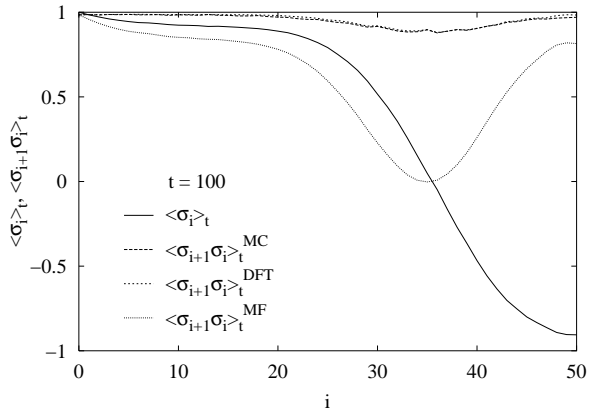


FIG. 5: Correlators  $\langle \sigma_{i+1} \sigma_i \rangle_t$  at  $t = 10^2$  from MC-simulation compared to correlators computed from TDFT and MF-theory, using the same MC spin density profile  $\langle \sigma_i \rangle_t$  as input. The TDFT-correlators are nearly indistinguishable from MC-correlators in this plot.

factorization of the last two terms in (22), gives quite different results (Fig. 4b). First of all, the overall process is much faster than in Fig. 4a. Second, within the region of the initial upspin domain it predicts a constantly decreasing plateau which is not observed in Fig. 4a. The origin of these failures of MF-theory becomes clear when we look at Fig. 5: Monte Carlo- and the almost identical TDFT-correlators  $\langle \sigma_{i+1} \sigma_i \rangle_t$  stay close to unity throughout the system, in contrast to the MF-factorization, and stabilize the respective spin configuration. Hence the relaxation process progresses only by a successive broadening of the interfacial region between the upspin and downspin domains and not by a decaying plateau.

## V. SUMMARY AND OUTLOOK

Applying a local equilibrium approximation to the master equation for atomic or spin configurations, kinetic equations for particle or spin densities were derived, which are compatible with the exact thermodynamics. The derivation was largely based on concepts from density functional theory. Kinetic equations obtained have the form of generalized “model B” or “model A” equations in the language of Ref. [17], where thermodynamic driving forces originate from the exact free energy functional. This “time-dependent density functional” (TDFT)-scheme is tested against Monte Carlo simulations for both a one-dimensional hopping model and the Glauber model, where the exact free-energy functional is known. Studying the dynamics of the interface between different domains, the TDFT yields excellent agreement with simulations with respect to density or spin density profiles and local correlation functions. The success of this theory appears to be a consequence of the fast relaxation of correlators towards their local equilibrium values.

Under the ultimate aim to develop theoretical tools for a description of phase transformation processes in real materials, several extensions of the present work are necessary. First of all, one needs reliable approximations for the free energy functional in higher dimensions. For two-dimensional lattice systems, a step in this direction has been taken recently [24], which was based on an extension of the techniques in Ref. [19]. Secondly, one would like to treat multicomponent systems. In that case, local equilibrium distributions of the type (1) may be insufficient to describe interdiffusion currents related to non-diagonal Onsager coefficients [6]. To incorporate such effects into the TDFT-scheme is an open question which deserves further study.

## Acknowledgment

The authors are grateful to J. Buschle for helpful conversations. H.L.F. was supported by NSF Grant DMR 9628224 and the Humboldt foundation. This work was supported in part by the Deutsche Forschungsgemeinschaft (Ma 1636/2-1, SFB 513).

## Appendix: Derivation of generalized “model A”-equations

The derivation of Eq. (10) proceeds in steps with some similarity to Ref. [8]. In the present “non-conserved” case we start from the master equation for single spin flips, see e.g. Ref. [21], to obtain the time derivative of single-spin averages. Exact averages are in turn approximated by averages  $\langle \dots \rangle_t$  with respect to the local equilibrium distribution  $P^{(loc)}(\boldsymbol{\sigma}, t)$ , which has the same form as (1) apart from a sign change in the second term in the exponent. (This is because the auxiliary fields  $h_i(t)$  in (1) have the meaning of effective site energies, while they are taken here as effective magnetic fields.) In this way we arrive at

$$\frac{d\langle \sigma_i \rangle_t}{dt} = -2\langle w_i(\boldsymbol{\sigma}) \sigma_i \rangle_t. \quad (25)$$

The summation over all  $\boldsymbol{\sigma}$  in the definition of the average on the right-hand side of (25) involves a summation over  $\sigma_i = \pm 1$ , which we treat with the help of the detailed balance condition:

$$\begin{aligned} & \sum_{\sigma_i} \exp[-\beta(H(\boldsymbol{\sigma}) - h_i \sigma_i)] w_i(\boldsymbol{\sigma}) \sigma_i \\ &= \frac{1}{2} \sum_{\sigma_i} e^{-\beta H(\boldsymbol{\sigma})} w_i(\boldsymbol{\sigma}) [e^{\beta h_i \sigma_i} \sigma_i + e^{-\beta h_i \sigma_i} (-\sigma_i)] \\ &= \sum_{\sigma_i} e^{-\beta H(\boldsymbol{\sigma})} w_i(\boldsymbol{\sigma}) \sinh \beta h_i. \end{aligned} \quad (26)$$

In the last step we have used  $\sinh(\beta h_i \sigma_i) = \sigma_i \sinh(\beta h_i)$  and  $\sigma_i^2 = 1$ . To restore the expression for  $P^{(loc)}(\boldsymbol{\sigma}, t)$

we multiply and divide (26) by  $\exp(\beta h_i)$ . Finally, it follows from the form of  $P^{(loc)}(\boldsymbol{\sigma}, t)$  that single-spin averages and the fields  $\mathbf{h}(t)$  are connected by  $h_i(t) + h = \partial F / \partial \langle \sigma_i \rangle_t$ , which is analogous to (3). Here,  $F$  is the

intrinsic free energy as a functional of the spin density. Combination of these results with (25) yields (10) and (11).

- 
- [1] For recent reviews see “Materials Science and Technology Vol. 5: Phase Transformations in Materials” ed. by R.W. Cahn, P. Haasen and E.J. Kramer, (VCH Weinheim, New York, 1991).
- [2] K. Binder, *Z. Physik* **267**, 313 (1974).
- [3] For a review, see J.F. Gouyet, M. Plapp, W. Dieterich and P. Maass, to be published.
- [4] R. Kikucki, *J. Chem. Phys.* **60**, 1071 (1979).
- [5] Several reviews are contained in *Prog. Theor. Phys. Suppl.* **115** (1994).
- [6] M. Nastar, V. Dobretsov and G. Martin, *Phil. Mag. A* **80**, 155 (2000).
- [7] D. Reinel and W. Dieterich, *J. Chem. Phys.* **104**, 5234 (1996).
- [8] H.P. Fischer, J. Reinhard and W. Dieterich, J.F. Gouyet, P. Maass, A. Majhofer and D. Reinel, *J. Chem. Phys.* **108**, 3028 (1998).
- [9] W. Dieterich, H.L. Frisch and A. Majhofer, *Z. Physik B* **78**, 317 (1990).
- [10] For a review, see H. Löwen, *Phys. Rep.* **237**, 249 (1993).
- [11] M. Nieswand, W. Dieterich and A. Majhofer, *Phys. Rev. E* **47**, 718 (1993); M. Nieswand, A. Majhofer and W. Dieterich, *Phys. Rev. E* **48**, 2521 (1993).
- [12] D. Reinel, W. Dieterich and A. Majhofer, *Phys. Rev. E* **50**, 4744 (1994).
- [13] K. Kawasaki and J.D. Gunton, *Phys. Rev. A* **4**, 2048 (1973).
- [14] H. Grabert, *Springer Tracts in Mod. Phys.* **95**, ed. by G. Höhler (Springer-Verlag, Berlin, 1982).
- [15] A. Latz, *J. Phys. Cond. Matter* **12**, 6353 (2000).
- [16] J. Schofield and I. Oppenheim, *Physica A* **204**, 555 (1994).
- [17] P.C. Hohenberg and B.I. Halperin, *Rev. Mod. Phys.* **49**, 435 (1977).
- [18] For a review see J.K. Percus, *Acc. Chem. Rev.* **27**, 8 (1994).
- [19] J. Buschle, P. Maass and W. Dieterich, *J. Phys. A: Math. Gen.* **33**, L41 (2000).
- [20] J. Buschle, P. Maass and W. Dieterich, *J. Stat. Phys.* **99**, 273 (2000).
- [21] R.J. Glauber, *J. Math. Phys.* **4**, 294 (1963).
- [22] The Monte Carlo time scale is chosen such that one Monte Carlo step per particle corresponds to a time interval  $\Delta t$  equal to the inverse of the largest possible hopping rate in (8),  $\Delta t = (\alpha e^{\beta V})^{-1}$ . We take  $\Delta t$  as our time unit, so that the variable  $t$  becomes dimensionless. In subsection 4.2, the time unit is  $\Delta t = \alpha^{-1}$ .
- [23] R. Nassif, Y. Boughaleb, A. Hekkouri, J.F. Gouyet and M. Kolb, *Eur. Phys. J. B* **1**, 453 (1998).
- [24] J. Buschle, P. Maass and W. Dieterich, to be published.
- [25] J. Crank, “The Mathematics of Diffusion” (Clarendon Press, Oxford, 1975), chapter 10.6.